13th World Conference on Earthquake Engineering
Vancouver, B.C., Canada
August 1-6, 2004
Paper No. 33

HIGH PERFORMANCE PASSIVE HYDRAULIC DAMPER WITH SEMI-ACTIVE CHARACTERISTICS

Haruhiko KURINO[1], Yoshinori MATSUNAGA[2], Toshikazu YAMADA[3] and Jun TAGAMI[2]

SUMMARY

This paper presents an ingenious passive hydraulic damper for structural control with high performance equivalent to that of a semi-active damper. This damper maximizes or minimizes the damping coefficient by regulating the opening of a flow control valve housed in the device, and absorbs much of the structure's vibration energy than a conventional passive viscous damper. The remarkable feature of this device is that all the valve control is carried out autonomously utilizing the pressure balance between two hydraulic chambers without any outer power resources. First, we explain the self-regulating hydraulic mechanism. Second, we present the results of dynamic loading tests on a full-scale prototype device (maximum force: 2MN) under both sinusoidal waves and non-stationary seismic response waves. It is thus confirmed that the developed device has the expected excellent energy dissipation capacity, and that the damper's dynamic characteristics can be well simulated by a simple analytical model. Finally, we demonstrate the results of seismic response analyses using an MDOF building model, and discuss the control performance of the device.

INTRODUCTION

Various types of semi-active damping devices have recently been developed in the civil engineering field for controlling structures (Spencer, B. F. [1]). The variable oil damper or MR damper, which can control its damping coefficient, are typical examples, and some devices have recently been installed in actual buildings. The authors have already developed a semi-active oil damper that can change its damping coefficient between maximum and minimum using a solenoid valve (Kurino [2]). This semi-active oil damper system was successfully installed in several actual buildings, and its excellent performance beyond that of passive dampers has been verified through vibration tests conducted on one of these buildings (Kurino [3], Mori [4], Tagami [5]). Thus, the semi-active mechanism is a desirable feature for structural response control under large earthquakes because of its small energy consumption. However, it is also true that the semi-active damper inherently depends on a power supply, however small it might be. The actually developed damper described above automatically becomes a passive hydraulic damper when

[1] Principal Research Engineer, Kajima Corporation, Tokyo, Japan. Email: kurino@kajima.com
[2] Supervisory Research Engineer, Kajima Corporation, Tokyo, Japan.
[3] Deputy Director, Kajima Corporation, Tokyo, Japan.

the power supply is cut off. Such failsafe functions to cope with a power failure or sensor trouble are crucial for realizing a semi-active system for application.

In order to overcome above the disadvantages associated with a semi-active mechanism, a high performance oil damper with an ingenious hydraulic valve system is introduced here. This system autonomously controls the flow control valve opening between two hydraulic chambers utilizing the pressure balance between them without any outer power resources. The valves in this system are activated through the hydraulic power accumulated in a rather small buffer placed between the two hydraulic chambers, and produces a maximum or minimum damping coefficient based on the pressure balance between them. This interesting function can realize a dreamy high performance passive hydraulic damper equivalent to a semi-active damper which can absorb much more structural vibration energy than a conventional passive damper. First, we explain the self-regulating hydraulic mechanism. Second, we present the results of dynamic loading tests on a full-scale prototype damper (Maximum force: 2MN) under both sinusoidal waves and non-stationary seismic response waves. Finally, we demonstrate the results of seismic response analyses using an MDOF building model, and discuss the control performance of the device.

CONTROL STRATEGY FOR EFFICIENT ENERGY DISSIPATION

Maxwell-type Mechanical Model

A simplified analytical model of a variable damping device installed in a structure by connecting it with a brace or a wall is expressed as a series of variable dashpots and linear springs, i.e., a Maxwell model, as shown in Figure 1. k_b indicates the bracing frame's stiffness, k_d is the damper stiffness and $C(t)$ is the damper's damping coefficient. We assume that k_b and k_d are constant, and that $C(t)$ can be changed from virtually zero ($C_{\min}$) to a very large value ($C_{\max}$) by adjusting the valve opening of the oil damper. $C_{\min}$ is the damping coefficient when the valve is fully open and $C_{\max}$ is that when the valve is closed. Because of the nature of the hydraulic mechanism, $C(t)$ is positive in all cases.

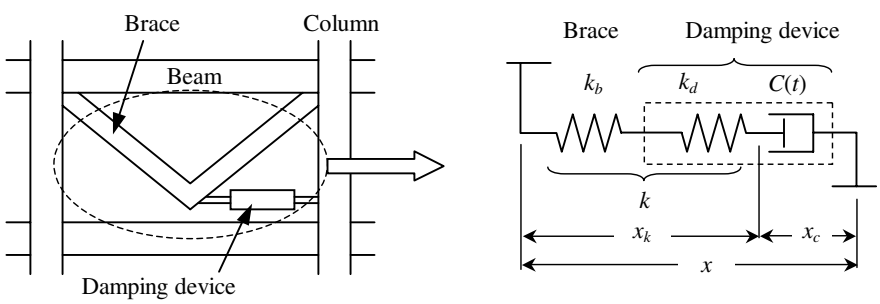

(a) Device installation (b) Maxwell type mechanical model

Figure 1. Mechanical model of installed damping device

Energy Dissipation Capacity of Passive Linear Damper

The energy dissipation capacity of a conventional passive damper, or a linear Maxwell model, under a harmonic motion $x=\delta\sin\omega t$ is maximized when the damping coefficient C(t) is set to a constant value k/ω. The maximum energy dissipated per cycle is

$$\Delta W = \frac{\pi}{2} k \delta^2 \tag{1}$$

Equation (1) is the index when discussing device performance.

Switching Control Law for Semi-active Damping Device

The control algorithm for maximizing the energy dissipation of a semi-active device is expressed by the following on/off or bang-bang control formula (Kurino [2]).

$$\begin{cases} F\dot{x} \geq 0 \;\; or \;\; |F| \leq F_0 & : C(t) = C_{\max} \\ F\dot{x} < 0 \;\; and \; |F| > F_0 & : C(t) = C_{\min} \end{cases} \tag{2}$$

The first term $F\dot{x}$ expresses the control power of the Maxwell damper. Figure 2 explains the energy dissipation process and the damper's behavior controlled by Equation (2). When the damper force and velocity directions are the same (from A to B), or the control power is positive, $C(t)$ is set to $C_{\max}$ to make the damper as stiff as possible. In this way, the device behaves just like a spring that accumulates the potential energy associated with spring stiffness and displacement motion. When the device motion changes direction (step C), or the control power becomes negative, $C(t)$ is switched to $C_{\min}$ in order to quickly dissipate the stored potential energy through viscous resistance within the damper valve. When the damper force is removed and becomes smaller than F_0 (step D), $C(t)$ is switched to $C_{\max}$ again.

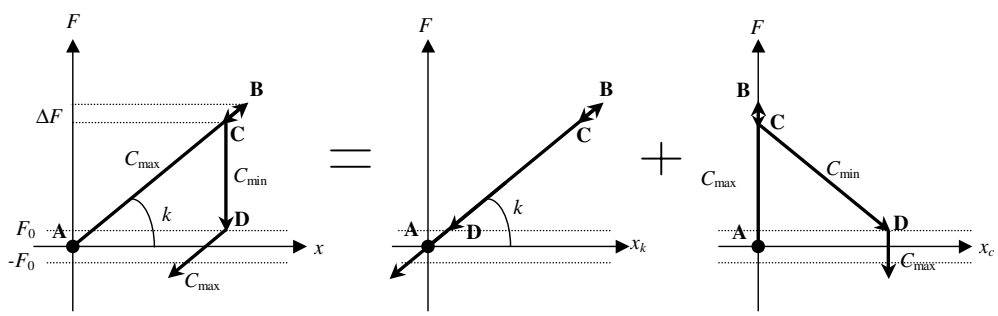

(a) Maxwell-model total (b) Spring element (c) Dashpot element

Figure 2. Principle and process of energy dissipation by control law Eq. (2)

Energy Dissipation Capacity of Semi-active Damping Device

Here we compare the semi-active damper's energy dissipation capacity controlled by Equation (2) with that of the conventional passive damper. Figure 3 (a) is an idealized force-displacement loop of the semi-active damper under a harmonic motion. It should be noted that this rectangular loop shape inherently associated with the switching control law is kept similar under any frequency or amplitude. If we assume that ΔF and F_0 in Figure 2 are virtually zero, the dissipated energy per cycle is

$$\Delta W = 4k\delta^2 \tag{3}$$

By comparing Equation (3) with Equation (1), we can see that the semi-active damper dissipates approximately two-and-a-half-times as much energy as the passive damper. The passive linear damper's maximum loop for $C=k/\omega$ is also shown in Figure 3(a) for comparison.

When assuming an MDOF structure under random excitations such as earthquakes, it becomes a little difficult. Figure 3 (b) explains the relations between damper force, story velocity, and story displacement of an MDOF structure under a seismic excitation. The block line shows the orbit when the story velocity is directly used for the control law of Equation (2). It is understood that the excessive frequent switching may be caused by higher mode components, and it is not the best strategy for maintaining a high energy dissipation rate. A possible solution is to use an appropriate compensating low-pass filter, and a concrete example is proposed by Kurino [2].

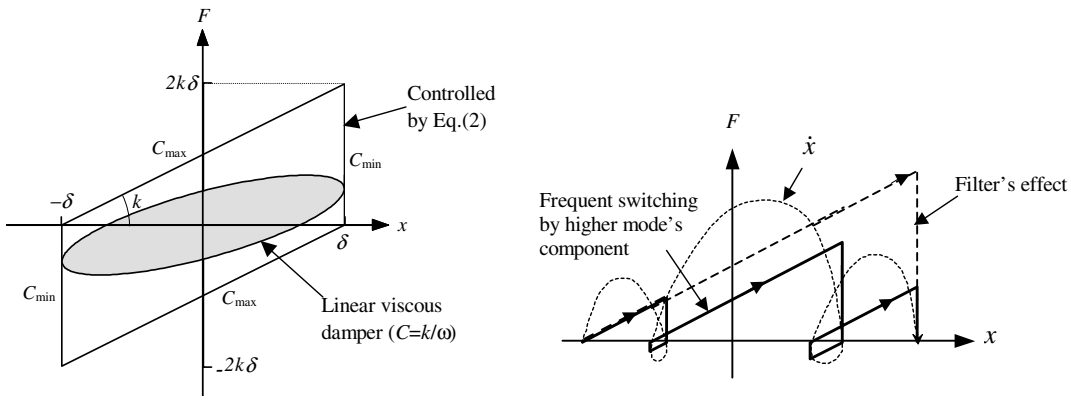

(a) Harmonic excitation (b) Random excitation

Figure 3. Relations between damper force and displacement

HYDRAULIC MECHANISM OF PROPOSED DAMPER

As discussed above, the semi-active damper controlled by Equation (2) realizes much more energy dissipation than a conventional passive damper. It would be very advantageous if the passive damper behaved just like a semi-actively controlled without needing any power supply. Here we propose an ingenious hydraulic mechanism that realizes a passive damper with semi-active characteristics.

The hydraulic circuit diagram is shown in Figure 4. This mainly consists of a logic type flow control valve (1) which directly controls the damping force between two hydraulic chambers, a kind of logic type pilot valve (2) which controls the back pressure of the flow control valve (1), and a buffer (3) which activates the pilot valve with accumulated hydraulic power. It is also equipped with a main relief valve (4) that limits the force generated under unexpected large motions. A buffer relief valve (5) is introduced in order to avoid functioning the flow control valve (1) when the main relief valve (4) works. The relief force of (5) is set a little smaller than that of the main relief valve (4). Other components, such as accumulator (6), stop valve (7), and check valves, are also installed with this valve system.

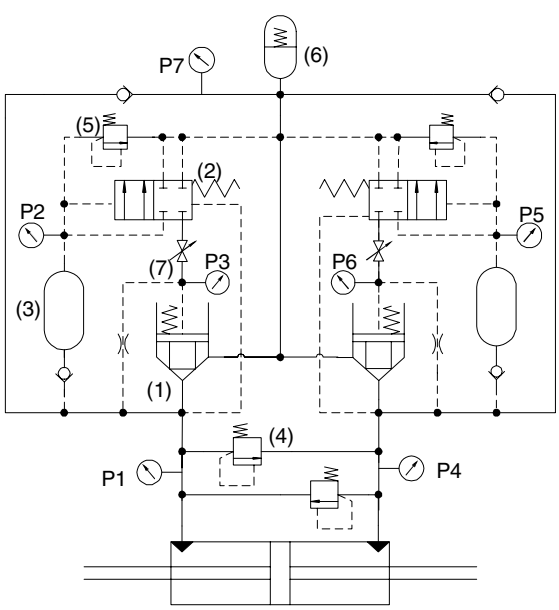

(1) Flow control poppet valve
(2) Pilot valve
(3) Buffer
(4) Main relief valve
(5) Buffer relief valve
(6) Accumulator
(7) Stop valve

Figure 4. Hydraulic circuit

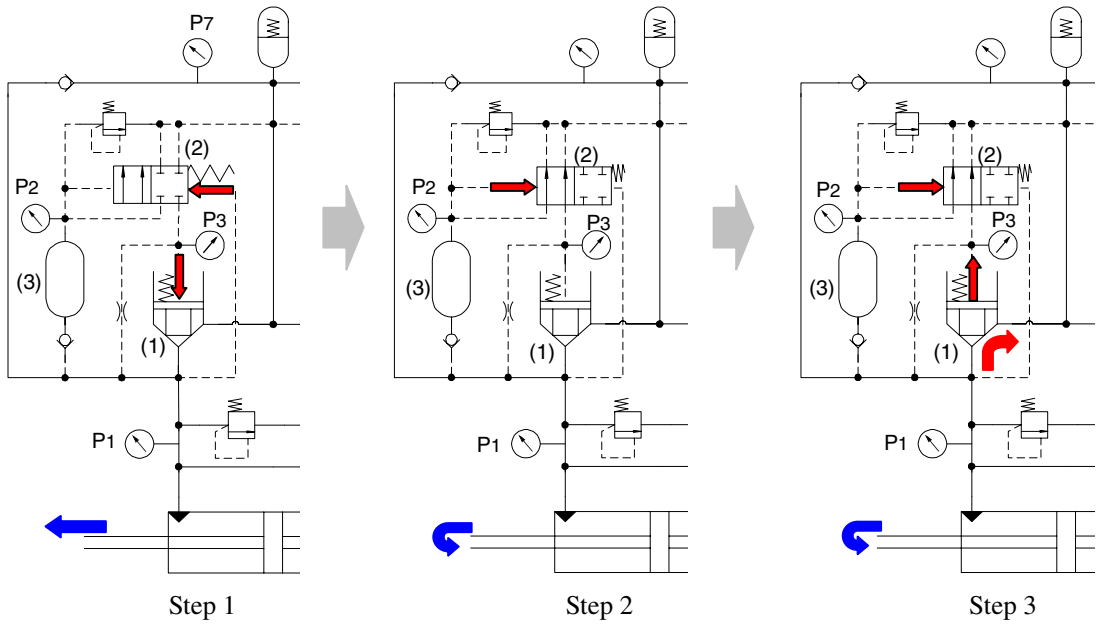

Figure 5. Principle and behavior of valve system

This hydraulic mechanism is most characterized by its simple utilization of pressure balance, making the hydraulic circuit work logically step by step. Figure 5 shows the conceptual hydraulic circuit status of these steps. Step 1 is when the hydraulic pressure at one of the chambers (P1) is increasing according to the piston motion, and this step corresponds to the region from A to B in Figure 2. In this step, the pilot valve (2) is closed due to the pressure balance between the two sides of the valve spool (P1 and P2), and the main flow control valve (1) is closed in the same manner as the pilot valve. During this step, the buffer (3) accumulates the pressure in it, and the buffer pressure P2 equals to P1. At step 2, corresponding to the point C in Figure 2, the cylinder pressure P1 begins to decrease. When P1 decreases to a certain extent, the pilot valve spool is moved by the accumulated buffer pressure P2, i.e. the pilot valve (2) opens. Then, the backpressure P3 begins to decrease, making the flow control valve (1) move. Finally, at step 3, the flow control valve (1) opens and the chamber oil rushes to the other side. When the cylinder pressure P1 is all removed, the flow control valve (1) and the pilot valve (2) are all closed again due to the pressure balance, and the accumulated buffer pressure is also removed. By repeating the above valve actions, the damper switches its damping coefficient according to the outer motion in the semi-actively controlled manner expressed by Equation (2). It is, however, noted that the filter logic for non-stationary disturbances mentioned before cannot be considered in this hydraulic mechanism. This is the only function omitted from the semi-active damper by Kurino [2]

FULL-SCALE PROTOTYPE DEVICE

In order to evaluate the logical motion of the proposed hydraulic circuit and the energy dissipation capacity, we developed a full-scale prototype damper. Figure 6 shows an outside view of the developed device equipped with the proposed hydraulic circuit, and Table 1 shows its specifications. The device is about 1.4m long and 1,000kg in weight, and has 2MN maximum force capacity. The major parts that contribute to generation of a large reaction force, such as a cylinder and a piston, are the same as those of previously developed passive dampers. The accumulator and the relief valve unit over and under the hydraulic valve block, shown in Figure 6, were added for the experiment. The hydraulic circuit is basically the same as the one in Figure 4. Seven channels of pressures, shown in Figure 4, are measured just for observation in the test.

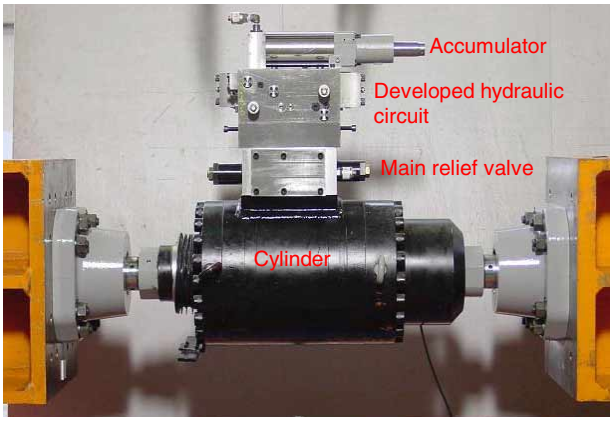

Figure 6. Outside view of full-scale device

Table 1. Specifications

Item	Specification
Maximum design force	2.0MN
Main relief force F_R	1.7MN
Maximum piston stroke	±60mm
Stiffness k_d	500MN/m
Size	ϕ 380×1410mm
Maximum pressure	35MPa

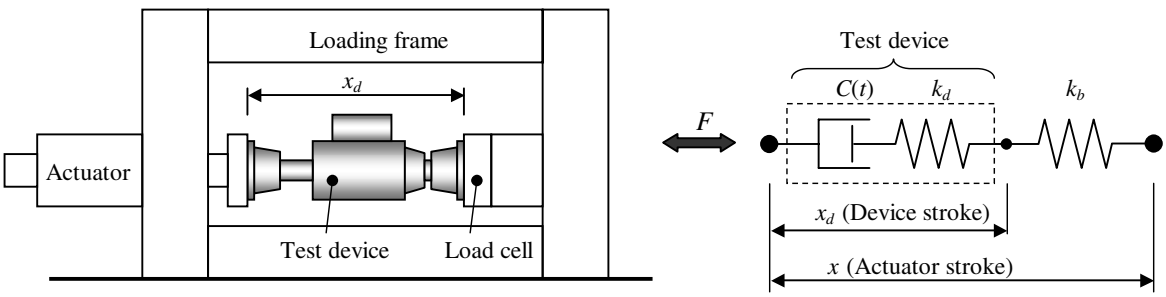

(a) Experimental setup (b) Mechanical model

Figure 7. Experimental setup and mechanical model

DYNAMIC LOADING TEST

Experimental Method

The loading setup is shown in Figure 7(a). A dynamic actuator is used for this test. Figure 7(b) shows a mechanical model of the experimental setup, and this is equivalent to the model in Figure 1(b) if k_b is assumed as the loading frame's stiffness. The actuator displacement is equivalent to the story displacement in actual building. We operate the actuator using a signal equivalent to the displacement between the stories in an actual building.

Test Results under Sinusoidal Loading

The force-displacement relations of the device obtained under sinusoidal loading for 0.3Hz, 0.5Hz and 1Hz are shown in Figures 8 and 9. Figure 8 shows the results when the stop valve (7) is closed for evaluation of the basic characteristics of the device and the test environment. Under this condition, the flow control valve (1) is closed compulsively, and the device behaves like a spring. The maximum damping coefficient evaluated from these test results is about 600MNs/m, and this is almost the same as the value for the semi-active damper using a solenoid valve (Kurino [2]). The identified device stiffness k_d and loading frame stiffness k_b are about 700MN/m and 620MN/m, respectively.

Figure 9 shows the results when the stop valve (7) is fully open, as originally designed. It is recognized that the characteristic rectangular loop associated with the control law of Equation (2) was accurately realized here. Although a little delay is observed at 1.0Hz, the expected valve operation was adequately

realized especially at 0.3Hz and 0.5Hz, which represent fundamental frequencies of high-rise buildings. Figure 10 shows the time histories of several measured pressures in the hydraulic circuit for 0.5Hz, ±2.0mm loading. It is observed that just after the pressures P1, P2, and P3 reached their peaks, the pilot pressure P3 drops quickly and the main pressure P1 is removed smoothly in a short time (about 0.1 sec). This is the expected logical motion of the proposed hydraulic circuit. The dissipated energy per cycle for 0.5Hz is almost 2.2 times as much as that theoretically expected for the linear viscous damper under the same stiffness condition. Thus, it is experimentally confirmed that the developed device equipped with the proposed hydraulic circuit realizes much more energy dissipation capacity than the conventional passive damper.

Figure 11 shows the results under rather large displacements. The dotted line shows the relief pressure of the buffer relief valve (5) in Figure 4. It is recognized that the flow control valve (1) opens only when the damper force becomes smaller than the buffer relief force. This function avoids operating the flow control valve (1) when the main relief valve (4) works.

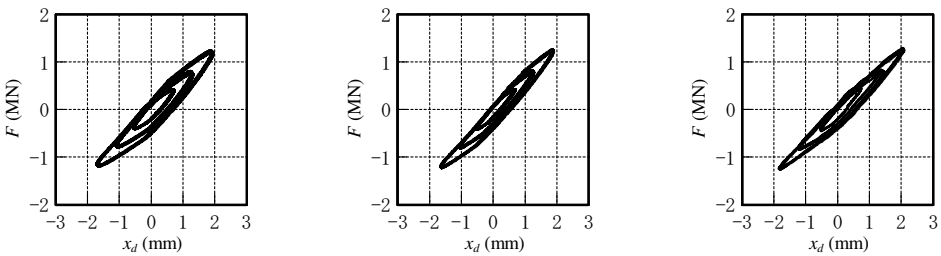

(1) 0.3Hz (2) 0.5Hz (3) 1.0Hz

Figure 8. Force-displacement relation for sinusoidal loading (valve (7) closed)

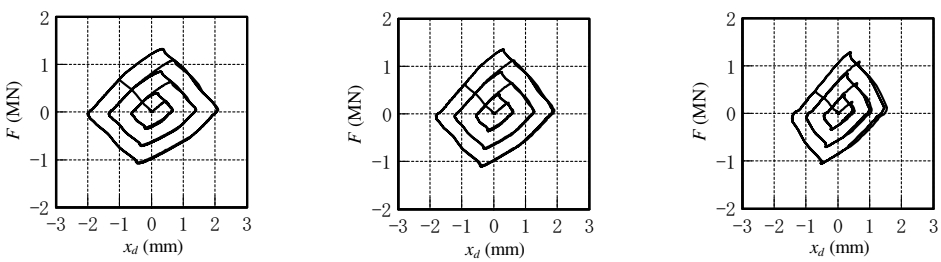

(1) 0.3Hz (2) 0.5Hz (3) 1.0Hz

Figure 9. Force-displacement relation for sinusoidal loading (valve (7) open)

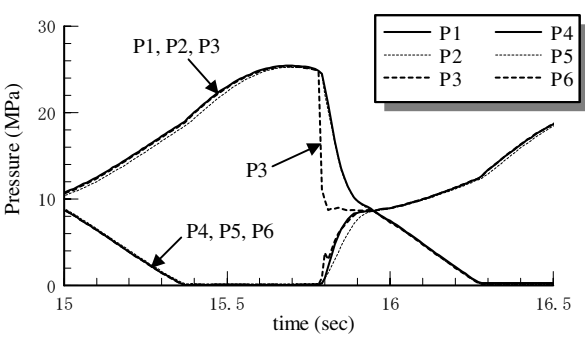

Figure 10. Pressure time history (0.5Hz)

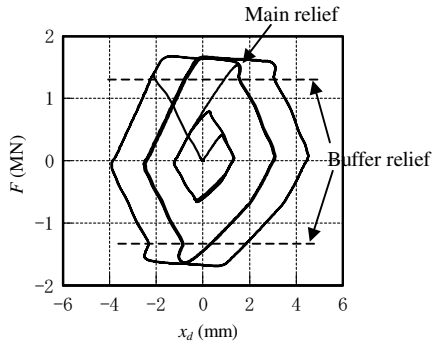

Figure 11. Force-displacement relation for large amplitude (0.3Hz)

Test Result under Seismic Response Wave Loading

To examine the dynamic behavior under non-stationary excitation, a dynamic loading test was conducted using the seismic response wave of a 30-story model for El Centro. Figure 12 shows the time histories of loading displacement, generated damping force, absorbed energy, and the force-displacement relation. It is confirmed that the damper force drops quickly when the loading displacement reaches its maximum. It is also confirmed that the valves operate stably based on the pressure balance even under such a complex loading condition.

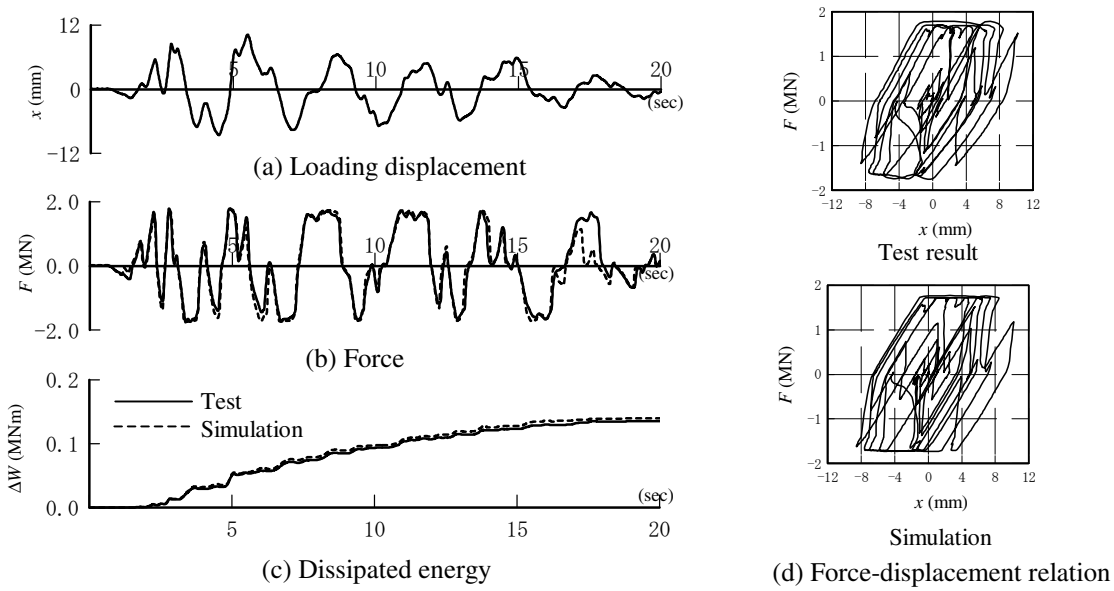

Figure 12. Test results and simulations for structural seismic response waves

System Evaluation

In order to evaluate the system feasibility, a simple analytical model was developed for structural response analyses. This macro-model simply changes the damping coefficient of the Maxwell model corresponding to the direction of the generated force. The buffer relief function is also considered here. The simulation results are also shown in Figure 12. The force-velocity characteristics of the Maxwell model's dashpot element are shown in Figure 13. The parameters used here are

Total stiffness $(k_b^{-1}+k_d^{-1})^{-1}$: 330MN/m
Main relief force F_R : 1.7MN
Buffer relief force : 1.4MN
ΔF (see Figure 2) : 20kN
F_0 (see Figure 2) : 50kN
Maximum damping coefficient C_{max} : 600MNs/m

Minimum damping coefficient C_{min} (Force-velocity relation when the flow control valve opens) is determined according to

$$F = \alpha\dot{x} + \beta\dot{x}^2$$

where α=5MNs/m, β=0.2MN(s/m)^2.

The simulation results agree well with the test results, and it is confirmed that the device's dynamic behavior can be accurately simulated with simple analytical parameters. This macro-model can easily be installed into a seismic response analysis program for structural design as a subroutine.

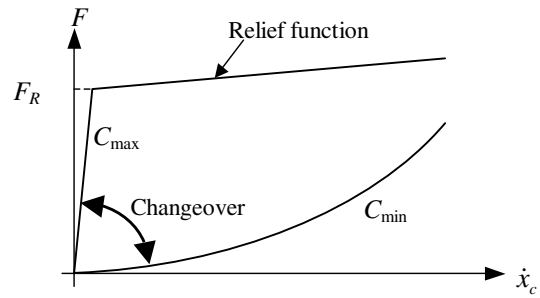

Figure 13. Force-velocity relation of dashpot element of macro model

Durability Test

Evaluation of stability and durability are crucial in the process for this kind of new system to be released to the market. The developed valve system showed great stability through the above dynamic loading tests and simulations. As the next step, a durability test of 53,000 cycles sinusoidal continuous loading (force level 300kN) was carried out for the same test device, and it worked perfectly during this test. It is confirmed that the developed valve system has excellent durability, and this damper can be applied to real buildings.

SEISMIC RESPONSE ANALYSIS OF MDOF STRUCTURE

Structure Model and Analytical Conditions

Structure Model

In order to evaluate the effectiveness of the developed damper, we conducted seismic response analyses using a 22-story building model. The total weight of the building was 30,000 ton, and Figure 14(a) shows a typical plan. We assume that two dampers are installed in each story (frames B and G), and only the short direction is considered in this study. Frames B and G are modeled as a bending-shear element as shown in Figure 14(b), and the other frames are modeled as a simple shear spring element. The damper portion is modeled as a Maxwell model, and is installed in the bending-shear element with a rigid bar. The first mode's natural period is 3.02 sec, and an initial structural damping ratio of 2.0% is assumed for the first mode. We give a bi-linear elasto-plastic hysteresis characteristic to the shear deformations of the bending shear element and the shear spring element.

We consider three damper conditions:

1. Open frame (without damper)
2. Linear viscous damper (conventional passive damper)
3. Proposed damper

Case 2 is when the damper is a conventional passive linear damper. The damping coefficient of each device is set to 50MNs/m based on the complex eigenvalue analysis. The damping ratio of the first mode in this condition is 5.5% including the initial structural damping of 2%. Case 3 is when the damper is the proposed device. The same analytical parameters evaluated in the above section were used in Case 3. The force limitation by the main relief valve is also considered here (1.7MN per device)

Input Earthquake

A simulated earthquake with a peak acceleration of 384.2 cm/s^2 is used here, and two different input levels, Level 1 and Level 2 (50% and 100% input) are considered. Figure 15 shows the acceleration time history and the response spectrum of the input ground motion (Level 2: 100% input).

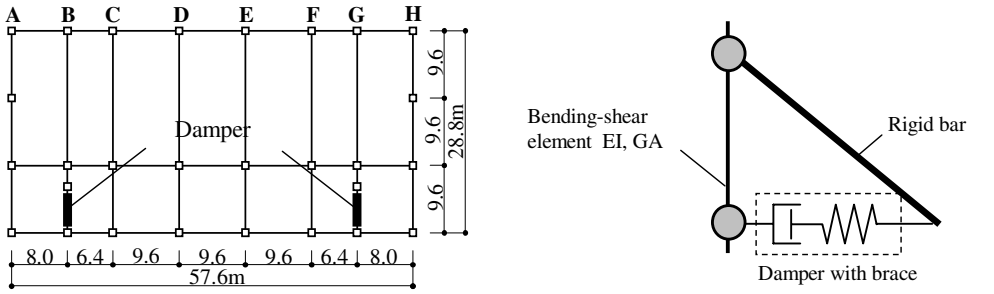

(a) Plan (b) Modeling of B and G frame

Figure 14. Building model

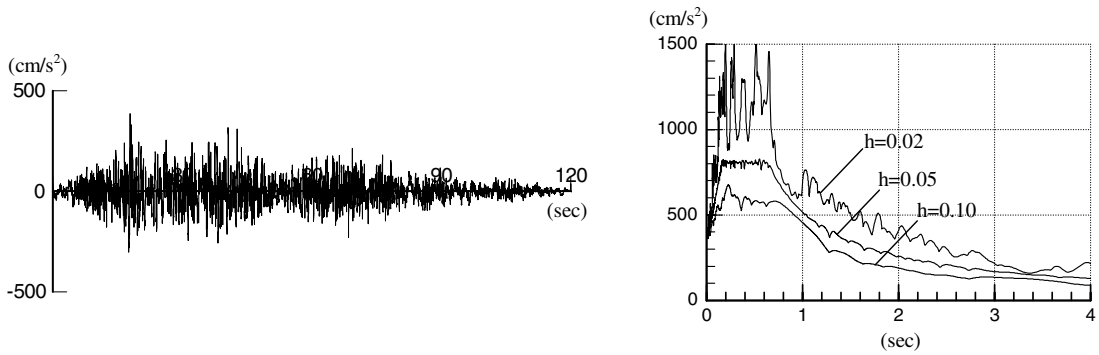

(a) Acceleration time history (b) Acceleration response spectrum

Figure 15. Input earthquake (Level 2 :100% input)

Analytical results

Level 1 (50% input)

Figure 16(a) shows the distribution of the frame's shear force for Level 1 (50% input). Although the linear viscous damper's response becomes approximately 20% smaller than in the open frame case, the proposed damper reduces the response by more 20% compared with the linear viscous damper. Figure 16(b) shows the displacement time histories of the top floor. The results for the open frame case and the proposed damper case are compared here. It is observed that the response displacement in the proposed damper case is kept small during the earthquake.

Level 2 (100% input)

Figure 17 shows the relations between the damper force and the story drift of the first floor for Level 2 (100% input). It is observed that the proposed damper generated much more control force than the conventional linear viscous damper, under a severe force limitation constraint (F_R=3.4MN per floor). Figure 18(a) shows the story drift angle, and (b) is the ductility ratio of the shear spring element that represents the structural frame. The reason why the difference between the linear viscous damper and the proposed damper become smaller than the result for Level 1 is the constraint of the damper's force capacity shown in Figure 17. Figure 18(c) indicates the distribution ratio of the input earthquake energy. Focusing on the open frame case, about 40% of the input energy is dissipated by the hysteretic energy of the frame. When the dampers are installed into the building, the frame's hysteretic energy is drastically reduced. The ratio of the damper's energy to the initial structural damping indicates the damping factor augmented by the damper. Although the energy dissipated by the conventional linear viscous damper is approximately 1.2 times of that of the initial damping, the proposed damper absorbs 1.8 times as much as the initial damping. These promising results confirm the feasibility and effectiveness of the proposed damper for actual application conditions.

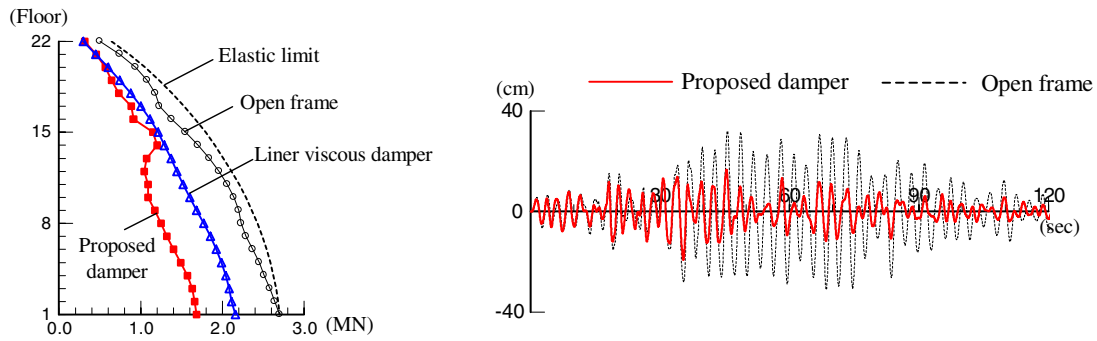

(a) Maximum frame shear force (b) Displacement time history of the top floor

Figure 16. Structural response for Level 1

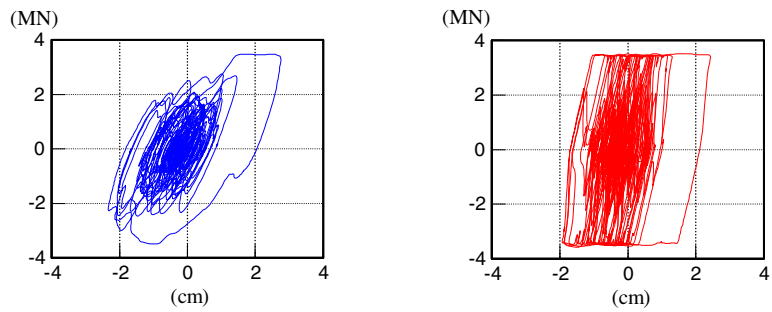

(a) Linear viscous damper (b) Proposed damper

Figure 17. Relation between damper force and story drift for Level 2 (1st floor)

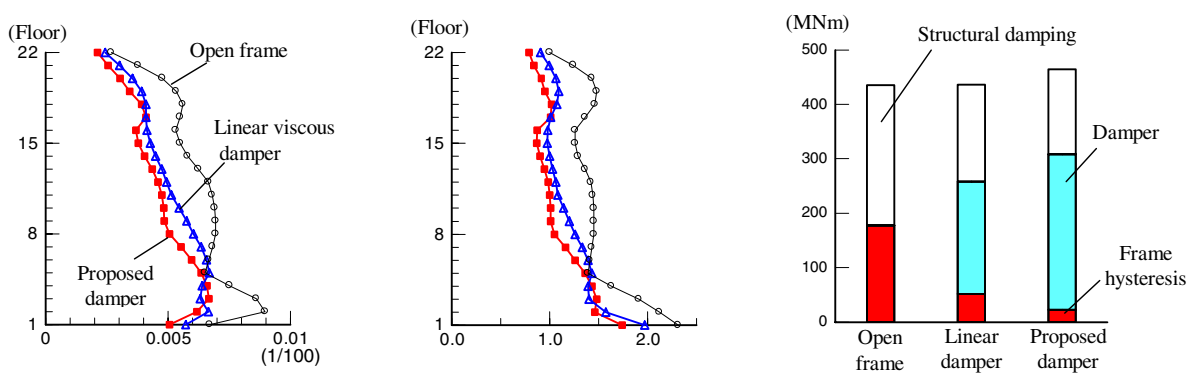

(a) Maximum story drift angle (b) Maximum ductility ratio (b) Distribution of input energy

Figure 18. Structural response for Level 2

CONCLUSION

We have presented a newly developed ingenious passive hydraulic damper for structural control with semi-active characteristics. This damper maximizes or minimizes the damping coefficient by regulating the opening of the flow control valve housed in the device utilizing the pressure balance between two hydraulic chambers without the need for any external power resources, and absorbs much more vibration energy than a conventional passive damper. Through dynamic loading tests conducted on the full-scale prototype device (maximum force: 2MN), the excellent energy dissipation capacity and durability are confirmed. It is also confirmed that the damper's dynamic characteristics could be well simulated by a

simple analytical model. In addition, we conducted seismic response analyses using an MDOF building model, and demonstrated the effectiveness of the proposed damper under actual application conditions. Thus, the proposed ingenious passive hydraulic damper has remarkable advantages, and we believe that it has wide applicability.

ACKNOWLEDGMENTS

The authors wish to express their appreciation to Mr. Sakai and Mr. Ichikawa of Toyooki Kogyo Co., ltd. and to Mr. Kotake of Hitachi Metals Techno, ltd. for their contribution to the production of the device.

REFERENCES

1. Spencer, B. F., Jr. and Nagarajaiah, S. "State of the Art of Structural Control", Journal of Structural Engineering, ASCE, 2003; 129(7): 845-856.
2. Kurino, H., Tagami, J, Shimizu, K. and Kobori, T. "Switching oil damper with built-in controller for structural control", Journal of Structural Engineering, ASCE, 2003; Vol.129(7): 895-904.
3. Kurino, H., Yamada, T., Tagami, J. and Shimizu, K. "Semi-active structural control by switching oil damper with built-in controller", Proc., Third World Conf. on Struct. Control, Como, Italy, 2002; Vol.1: 211-216.
4. Mori., F., Sugiyama, T., Suwa, M., Kurino, H. and Fukushima, I. "Application of semi-active switching oil damper to an actual 11-storey building", Proc., Third World Conf. on Struct. Control, Como, Italy, 2002; Vol.2: 143-148.
5. Tagami, J., Koshida, H., Kuirno, H., Sugiyama, T., Suwa, M. and Mori, F. "Forced vibration test of an 11-storey building with semi-active switching oil damper", Proc., Third World Conf. on Struct. Control, Como, Italy, 2002; Vol.2: 75-80.